INVESTIGATING SPACE BRAIN: HOW DO BRAIN CELLS RESPOND TO THE EFFECTS OF INCREASED INTRACRANIAL PRESSURE?

Carly Norris[1,2], Susan Murphy[2], Allison Nelson[1,2], Justin Weatherbee[2], Pamela VandeVord[1,2,3]

1. *Virginia Tech, Department of Biomedical Engineering and Mechanics, Blacksburg, VA*
2. *Virginia Tech, School of Biomedical Engineering and Sciences, Blacksburg, VA*
3. *Salem Veteran Affairs Medical Center, Salem, VA*

Abstract

Recent research suggests that astronauts experience neurological deficits while in space and upon their return. Such changes include neuroinflammation and oxidative stress, which can lead to cognitive decline if not treated. However, the sample sizes for these findings are low and the cause of such damage could be due to a number of factors during flight, including extended effects of microgravity and radiation or exposure to large magnitude accelerations. Strategies need to be implemented to determine the extent of neurological damage and address these deficits with appropriate therapeutic approaches. In this work we outline methods and guidelines for determining injury severity following exposure to impulses of varying magnitude using a preclinical model. We then optimized the quantification of amino acids within the brain using high performance liquid chromatography as an acute measure that can be correlated to intracranial impulse. Lastly, we compare the neurochemical changes at 24 hr following the impulse event. Future work will develop time-course profiles of amino acids for defined injury severities to optimize therapeutic targets so that the neurological safety of our astronauts can be addressed.

Introduction

The brain undergoes extensive compensatory mechanisms during spaceflight and upon return to Earth where recent studies are finding that the neurological health of astronauts may be at risk. Specifically, adaptive responses to microgravity and radiation have shown deficits in neuronal integrity leading to inflammation and cognitive decline, defined as space brain[1, 2]. Further side-effects of microgravity result in increased intracranial pressures (ICP) due to fluid shifts while in space. Vision impairment, vertigo, headaches, and numerous other neurological symptoms have been linked to this increased ICP and the pathophysiology resulting from these changes remains unclear[3, 4]. Physiological adaptation to microgravity and then back to full gravitational forces occurs following high impulse take-off and landing events, respectively, imparting additional stresses and strains on the brain and thus complicating this already complex problem. It is important to account for the metabolic stress that occurs in response to the increased ICP, stresses, and strains imparted on the brain tissue. ICP has long been known as a correlate for brain injury severity[5, 6], however many injury models investigate ICP increase following blunt trauma, which does not mimic the events occurring during space travel. In this work we generate high impulse overpressure environments where we aim to measure the resulting ICP magnitude and duration experienced in the brain tissue and correlate these to severity of neurological deficits seen in other traumatic brain injury models.

We then aim to quantify changes in neurochemical concentrations of amino acids at acute time points. The acute metabolic regulation of amino acids in response to increased ICP is critical in the assessment of neurological health as dysregulation leads to secondary response mechanisms and contributes to further injury response cascades. For instance, in a

healthy brain, concentrations of Glutamate (Glu), an excitatory neurotransmitter, are balanced by γ-Aminobutyric acid (GABA), an inhibitory neurotransmitter. When this ratio of Glu:GABA increases, the neuronal cell becomes excitotoxic, leading to cell death[7]. Of particular interest are the metabolic cycles such as, the Glu–Glutamine (Gln) cycle[8], GABA-Gln cycle[9], and the conversion of Aspartate (Asp) to Glu in the α-ketogluterate cycle[10]. Each plays a key role in maintaining homeostasis and concentrations of these free amino acids can depict the extent of metabolic stress the cells are experiencing. While significant changes in neuronal regulation of GABA was previously identified following proton irradiation, using concentrations controlled to mimic those experienced during space travel[11], this model does not take into account metabolic regulation related to changes in ICP. This work optimized methods quantifying amino acids within the brain for defined static overpressure magnitudes and analyzed profiles in the hippocampus at 24 hr following the high impulse event. Future work will expand on amino acid profiles at various time points for the identification of potential therapeutic targets. With this method of detecting response profiles, we expect accelerated prophylactics and/or treatments for men and women affected by space brain, thus accelerating us to Mars where the risk of long-term neurological deficits are mitigated.

Methods

Preclinical Model

Male Sprague Dawley rats were purchased from Envigo and all procedures were performed using an established animal model following approval from the Virginia Tech Institutional Animal Care and Use Committee. The animals were acclimated for at least three days and followed a 12 hour light-dark cycle with food and water administered *ad libitum*. Two main experiments were performed to: 1) measure intracranial pressure for a range of high impulse events and 2) optimize and quantify amino acid response 24 hr following the high impulse event.

High Impulse Event

To generate a non-impact, high impulse event, we used a 10 ft long Advanced Blast Simulator (ABS) located at the Virginia Tech Center for Injury Biomechanics (CIB). A blast wave was directed along a rectangular test section (1 ft x 1 ft) and the impulse was then absorbed by an end wave eliminator to keep potential wave reflections from hitting the specimen of interest (**Fig. 1**). The blast wave was driven by compressed helium, and peak static overpressure was controlled by the thickness of the acetate membrane between the driver and the transition section. Static overpressure is measured in three locations along the wall of the test section using piezoelectric sensors. This preclinical injury model is described in more detail in Cho et al. (2013)[12].

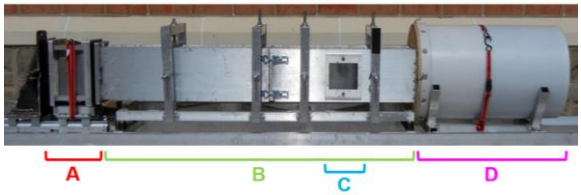

Figure 1. Advanced Blast Simulator. A) Driver section where compressed gas builds. B) Sloped transition section followed by rectangular test section. C) Location of test specimen. D) End wave eliminator.

Measuring Intracranial Pressure

Stainless steel pressure transducers (M060) were purchased from Precision Measurement Company (Ann Arbor, MI) with a diameter of 1.52 mm rated to withstand overpressures up to 3400 kPa. ICP and wall pressure transducer signals were conditioned and acquired at 800 kHz using a TMX Multi-Channel High Speed Data Acquisition Recorder (AstroNova Inc., West

Warwick, RI). Cables were shielded using braided sleeving and grounded to the data acquisition system.

Subjects were transported from the animal facility to the CIB where the surgical procedure, high impulse events, and euthanasia occurred. The rats (n = 9, 81.4 ± 7.1 days, 316.6 ± 20.3 g) were briefly anesthetized with 4% isoflurane prior to administration of ketamine/xylazine (80 mg/kg / 10 mg/kg). Intracranial surgery was performed through the occiput to minimize interference with the head-on blast wave. Once stabilized in a stereotaxic frame, a vertical incision was made along the back of the scalp exposing the occiput and surrounding musculature. Hydrogen peroxide was used to clean the skull, followed by acetone to degrease the surface. Surrounding musculature was then coated with Vetbond (3M) to control bleeding. A stereotaxic high-speed drill was used to drill a 2 mm hole in the right side of the occiput. Great care was taken not to damage vasculature once the hole was established. The M060 transducer was then inserted parallel to the top of the skull using a 15 gauge, 10 mm long guide cannula (P1 Technologies Inc.) (**Fig. 2**). The guide cannula was removed while the sensor was held in place. Directly to the left, a surgical screw was placed to stabilize the pressure sensor. The hole surrounding the gauge was filled using a viscous acrylate resin (Insta-Cure+) and after full cure, the sensor was tugged to ensure a closed system. The scalp was then sutured shut and reinforced with Vetbond. To prevent snagging and removal of the sensor during the high impulse event, the sensor was sutured to the skin on the upper neck and the torso to secure the shielded wires.

Subjects were suspended within the test section in a taut mesh sling that was secured to the top and bottom of the ABS to reduce movement during the impulse event. The subjects were oriented facing the driver compartment and extra padding was inserted to reduce relative motion inside the sling. The braided sleeving protecting the M060 transducer was taped along the length of the test section and exited the tube just before the end wave eliminator. The subjects were then exposed to four impulse events where the target positive impulses were: 30 kPa*ms, 50 kPa*ms, 80 kPa*ms, and 110 kPa*ms. The experiment was replicated three times, thus each subject was exposed to a total of 12 events. Euthanasia immediately followed the final blast exposure and brain tissue was harvested to confirm sensor placement by Hematoxylin and Eosin (H&E) stain (Abcam).

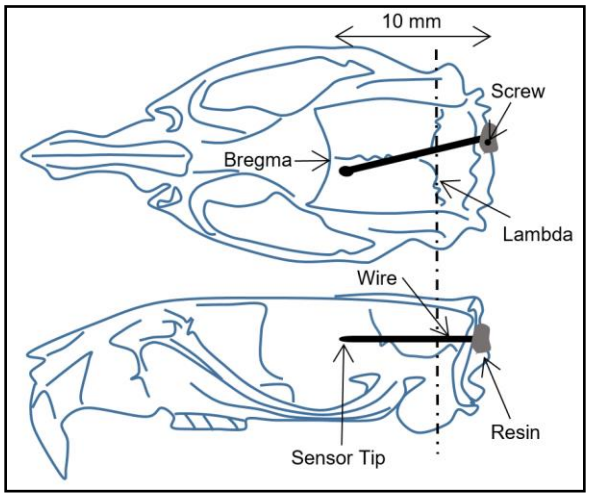

Figure 2. Stereotaxic reference for sensor and screw placement.

Data was processed in MATLAB (Mathworks, Natick, MA) where a 6th order low-pass Butterworth filter was applied with a cutoff frequency of 16500 Hz. Positive impulses for both static overpressure and intracranial pressure, defined in **Figure 3**, were then quantified (**Table 2-3**).

HPLC Optimization

High performance liquid chromatography (HPLC) methods were optimized to the following criteria, adapted from Zhang et al. (2013)[13]:

Table 1. Optimized HPLC methods for amino acid analysis.

Mobile phase	76.5% 75 mM Phosphate buffer, pH 6.3, 20% Methanol, 3.5% Acetonitrile
Analytical column	C18 Hypersil™ 3 µm BDS 3 mm × 150 mm
Guard cartridge	Universal Uniguard Holder 3 mm i.d.
Flow rate	0.4 mL/min
Column temperature	45 °C
Voltage	550 mV
Derivatizing agent	27 mg of OPA; 1 ml of methanol; 9 mL of 0.2 M H_3BO_3 and 5 µL of C_2H_6OS (βME)
Calibration method	External Standard
Type of detection	Electrochemical detection
Run time	28 min
Analytes quantified	Ala, Arg, Asp, Ser, Tau, Thr, Glu, Gln, Gly, GABA
Sample	Amino acids extracted from rat brain

Amino Acid Extraction and Quantification

To investigate the neurochemical response at 24 hours following a high impulse event, non-instrumented subjects were exposed to a single event (128.6 ± 6.5 kPa) and then euthanized 24 hours later (n = 5, 76 days, 315.2 ± 9.0 g). Control subjects underwent all experimental procedures except for the impulse event (n = 4, 76 days, 320.25 ± 10.9 g).

Brain tissue was quickly extracted (< 2 min), rinsed with 0.9% saline solution, and placed on ice for dissection. Regions of interest were stored in centrifuge vials on dry ice and transported to long term storage at -80°C. Tissue mass in each vial was recorded. This tissue was then diluted with 500 µl of deionized water and homogenized. The samples were centrifuged twice at 10,000 rpm, 4°C for 20 min. The samples were then centrifuged through a 0.22 µm filter (Costar Spin-X) at 10,000 rpm, 4°C for 20 min to isolate the free amino acids. Lastly, 10 µls was diluted in 990 µls of deionized water and placed in the autosampler rack at 6°C to slow degradation as much as possible. Samples were loaded into the rack one at a time to prevent degradation over the full sequence run time.

Stock solutions were prepared individually by dissolving 30 mg of each amino acid into 10 mL deionized water. These concentrations were aliquotted into vials and stored at -80°C until use. The standards were then thawed and four µls of each stock solution (40 µl total) was diluted with 1.960 ml deionized water. The standards were then serially diluted four times, and each standard concentration was placed in the autosampler rack at 6°C. Calibration curves and regression coefficients for each standard were determined (**Table 4**). The concentration of each amino acid was then quantified in µg per g of tissue based on these calibration curves.

Results

Intracranial Pressure Response

The ABS static overpressure traces followed the Friedlander waveform (**Fig. 3**), and positive impulses calculated from the static overpressure traces, in **Table 2** demonstrate that the static overpressures for each subject were controlled and repeatable. However, in **Table 3**, while intracranial impulses increase as static overpressures increase, results are inconsistent across animals.

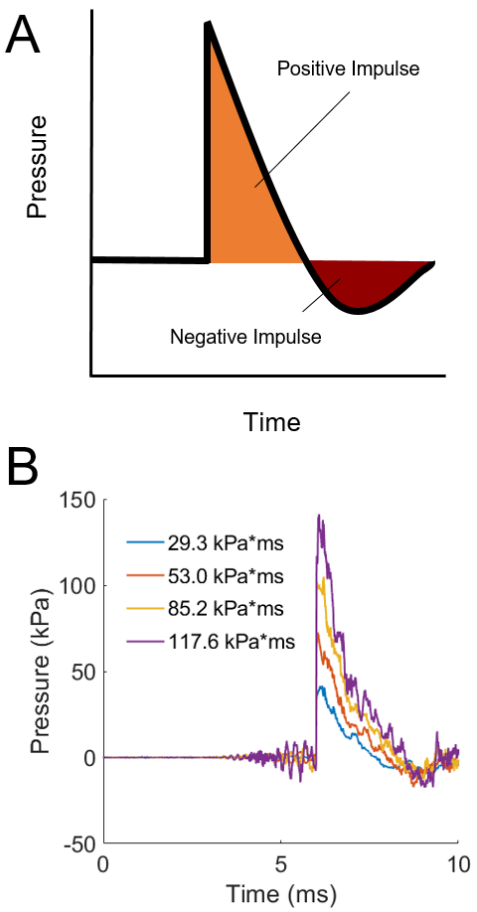

Figure 3. A) Friedlander waveform. B) Representative static overpressure traces for a single subject.

Table 2. Average positive impulse of the triplicate static overpressure events ± standard deviation.

Subject #	30 kPa*ms	50 kPa*ms	80 kPa*ms	110 kPa*ms
1	30.5 ± 1.1	52.8 ± 2.2	73.1 ± 5.6	114.4 ± 7.1
2	32.4 ± 2.0	51.6 ± 4.6	79.1 ± 16.3	124.5 ± 0.8
3	43.5 ± 12.6	57.9 ± 3.8	85.5 ± 6.2	102.8 ± 12.3
4	36.4 ± 2.1	57.2 ± 4.1	82.1 ± 4.5	112.1 ± 3.7
5	35.6 ± 2.8	51.3 ± 3.8	72.7 ± 3.1	109.7 ± 2.6
6	36.6 ± 1.5	54.6 ± 2.1	81.6 ± 5.5	111.5 ± 4.0
7	34.0 ± 1.8	59.5 ± 4.2	78.0 ± 7.8	122.6 ± 1.6
8	32.3 ± 4.6	55.9 ± 3.0	82.0 ± 14.9	107.1 ± 7.4
9	34.4 ± 4.9	51.1 ± 3.8	80.6 ± 10.0	114.3 ± 5.3

Table 3. Average positive impulse of the triplicate intracranial pressure events ± standard deviation.

Subject #	30 kPa*ms	50 kPa*ms	80 kPa*ms	110 kPa*ms
1	166.7.5 ± 67.6	190.8 ± 66.9	131.7 ± 50.6	158.9 ± 27.9
2	268.6 ± 71.5	418.7 ± 49.4	260.6 ± 93.0	285.8 ± 40.8
3	239.4 ± 193.6	245.7 ± 121.8	152.6 ± 42.6	251.9 ± 62.3
4	65.3 ± 12.0	119.8 ± 53.9	291.7 ± 15.1	238.1 ± 63.2
5	24.2 ± 13.5	45.8 ± 38.5	72.9 ± 3.4	120.4 ± 19.1
6	38.6 ± 2.1	42.1 ± 1.2	47.8 ± 0.8	62.3 ± 7.7
7	36.4 ± 2.7	84.6 ± 10.0	121.0 ± 15.1	182.4 ± 7.4
8	30.4 ± 7.0	45.2 ± 5.0	63.1 ± 7.9	70.2 ± 5.0
9	50.6 ± 5.6	53.2 ± 16.6	73.6 ± 9.3	105.6 ± 3.9

In many cases, this is due to M060 sensor malfunction. **Figure 4** shows examples of erratic spikes from the sensors that led to corrupt data. This includes examples where the ICP is amplified significantly beyond the static overpressure (**Fig. 4A**), and sharp negative spikes immediately follow sharp positive spikes, which reach near impossible vacuum pressures, in the middle of the anticipated impulse region (**Fig. 4B-Fig. 4C**). While the positive impulse in **Figure 4D** follows the static overpressure as expected, the negative impulse still reaches values outside reasonable limits.

Nevertheless, in cases such as Subject 9 for example, the ICP traces follow expected trends shown in Leonardi et al. (2011)[14] and Bolander et al. (2011)[15] where the peak ICP is directly correlated to incident overpressure and the energy transferred to the brain tissue through skull flexure is represented by the frequencies of the positive ICP impulse (**Fig. 5**). ICP baselines are re-established within 2 ms of exposure, however, this is not the same story for neurochemical concentrations.

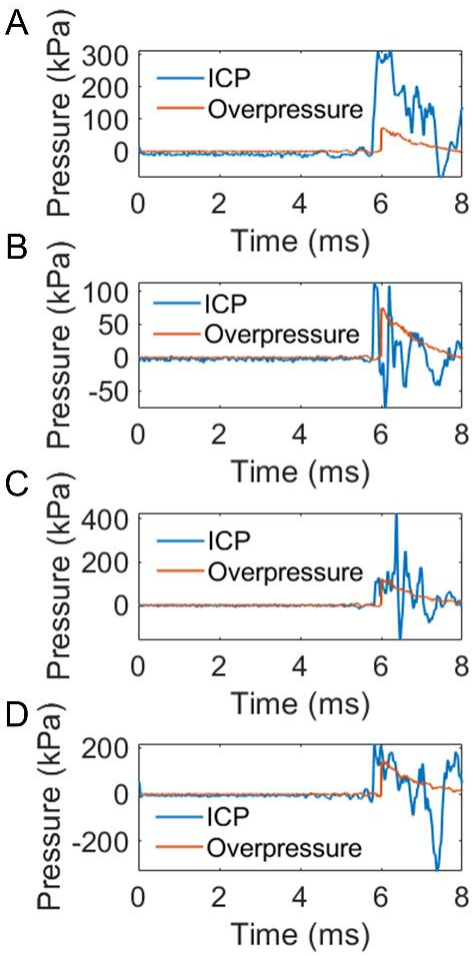

Figure 4. Examples of corrupt ICP response with M060 pressure transducers. A) The ICP trace is two orders of magnitude greater than the overpressure, indicating an amplified signal. B) The trace follows the expected trend of the ICP impulse, however it seems there is an underlying frequency and erratic amplitude spiking. C) Initial ICP trace follows the expected trend, but is interrupted by a phantom signal of large magnitude. D) Signal follows expected positive impulse, however negative impulse is beyond vacuum pressure.

Sensor placement was confirmed for each subject using H&E staining methods. It was found that in most cases, even though the sensor was placed in the right occiput, it angled medially towards the ventricles or laterally to the left (**Fig. 6**). As mentioned in Leonardi et al. (2011)[14], peak pressures in the ventricles are less than those in tissue, however, ventricle readings were more consistent. The location of the sensor tip is a critical control measure which could account for intersubject variability.

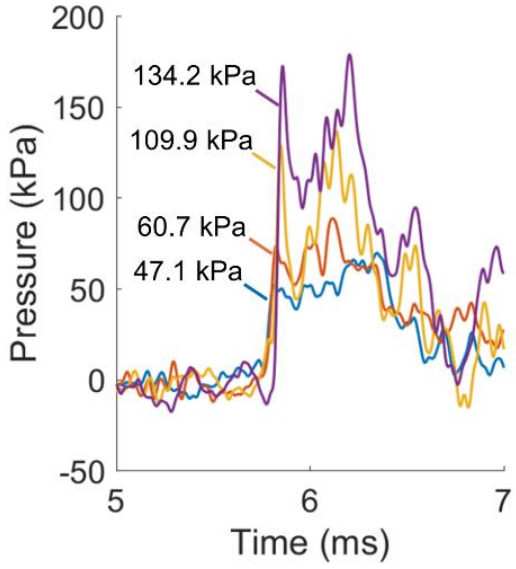

Figure 5. ICP traces for increasing incident static overpressures of 47.1, 60.7, 109.9, and 134.2 kPa in Subject 9.

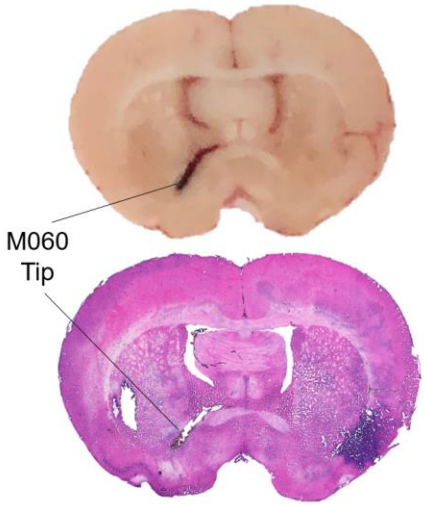

Figure 6. Confirmed location of M060 sensor tip in the left anterior commissure of Subject 9 where the tissue is frozen in a sucrose solution (top) and stained using H&E techniques (bottom).

Neurochemical Response

Optimization of HPLC methods resulted in the chromatogram in **Figure 7** where 10 amino acids of interest are separated and identified: Aspartate (Asp), Glutamate (Glu), Serine (Ser), Glycine (Gly), Glutamine (Gln), Threonine (Thr), Taurine (Tau), Alanine (Ala), Arginine (Arg), and GABA. Regression coefficients from the calibration curves in **Table 4** all exceed 0.99, indicating exceptional sensitivity to changes in amino acid concentrations for each analyte of interest.

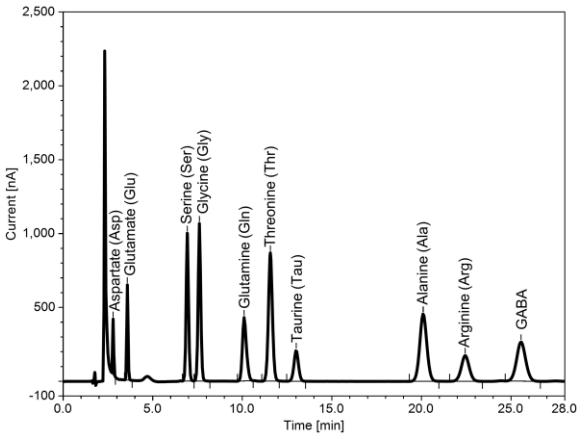

Figure 7. A representative chromatogram of 10 amino acid standards (3 mg/mL).

Table 4. Regression coefficients of calibration curves for each standard.

Standard	R^2	Standard	R^2
Asp	0.9951	Thr	0.9997
Glu	0.9986	Tau	0.9982
Ser	0.9994	Ala	0.9999
Gly	0.9999	Arg	0.9997
Gln	0.9986	GABA	0.9996

The neurochemical response of all 10 analytes were quantified in the hippocampus at 24 hr following the high impulse event. The hippocampus was selected as a region known for its sensitivity to metabolic changes, where neuroinflammation and neurodegeneration have been quantified in this model previously at 24 hr[16]. Following high impulse event, there was an increase in Glu and a decrease in GABA, resulting in a significant increase in the Glu:GABA ratio (p=0.05) (**Fig. 8C**). Further, the increased Gln (p=0.08) and Asp indicate an excess excitatory presence and thus increased metabolic demand.

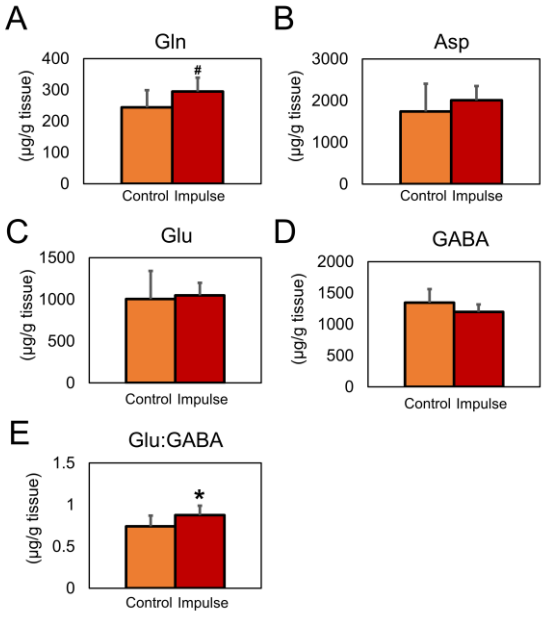

Figure 8. Amino acid concentrations normalized to tissue weight 24 hr following high impulse event. A) Average increase in Gln (#p = 0.08). B) Average increase in Asp. C) Average increase in Glu. D) Average decrease in GABA. E) Significant increase in Glu:GABA (*p = 0.05).

Discussion

ICP impulse and magnitude increased with increasing static overpressure, the HPLC methods separate and quantify the metabolites with high sensitivity, and metabolic stress was identified at 24 hours following high impulse event.

While the piezoelectric wall sensors demonstrated repeatable overpressure measurements within the ABS, it is apparent

that the inconsistencies in the M060 sensor ICP measurements make them unreliable as a correlate for severity of tissue disruption. The disagreement in positive ICP impulses between Subjects 1-4 and Subjects 5-9 warranted further investigation. The M060 sensors were tested in the ABS at various orientations and it was determined that they are not suitable in such high impulse environments. Future work will incorporate different pressure gages that have been tested and approved for high impulse scenarios[17]. Additional efforts will also be made to control the angle of sensor insertion.

Metabolic stress was identified in the hippocampus at 24 hr where increased Glu:GABA could indicate excessive excitability of the neurons. Over-excitability leads to an excess of Glu, yet only a marginal increase was observed. Nevertheless, this data shows a more significant increase in Gln, indicating that the astrocytes are effectively converting excess Glu to Gln. With an excess Gln and Asp, inhibitory neurons should be able to generate more GABA, but without the proper energy stores, it is projected that these components are not used up and GABA is not generated fast enough to properly balance the excess excitability[18]. Thus, it is likely that in this case energy stores are being depleted. Without enough energy to regulate membrane potential, excitability may become exacerbated and be the cause of detected neuroinflammation and neurodegeneration.

A similar injury model to this design is blast-induced traumatic brain injury (bTBI) where a high impulse event occurs without blunt force trauma and the brain undergoes metabolic stress. One study used magnetic resonance spectroscopy (MRS) to quantify metabolites in *ex vivo* hippocampal tissue at 24 hr following bTBI where they found a decrease in GABA, however, there was also a significant decrease in Glu[16]. Another study that quantified metabolites using MRS on *ex vivo* hippocampal fluid extracts at 24 hours following bTBI saw a significant increase in Asp and GABA and significant decreases in Glu and Gln[19]. Provided that these studies show conflicting results with each other as well as the results shown in **Figure 8**, further work should be done using a more sensitive, controlled, approach, such as HPLC.

The results in **Figure 8** most closely align with results from an impact model for mild traumatic brain injury where they found trends of increases in Glu and Gln at 24 hr and significant increases in Asp and GABA using HPLC methods[20]. In this case, the increase in GABA is likely an over-compensation for the initial excitability that occurred prior to this 24 hr assessment. It is expected that pathophysiology from non-blunt injuries would differ. Future work will focus on the development of a temporal profile for amino acids at 1 hr, 4 hr, 24 hr, and 48 hr after insult. These are expected to aid in the distinction between the response to blunt impact versus high impulse event. Furthermore, it is critical to continue this work towards understanding the pathophysiology of non-impact injuries in the context of space travel.

This work demonstrates repeatability of the high impulse events and drives the need for further investigation of the metabolic response at various time points. Once these profiles are developed *ex vivo*, the metabolic response has the potential to be investigated *in vivo* using MRS in humans to determine stage of metabolic stress and allow doctors to effectively treat their patients.

Conclusion

ICP impulse was directly correlated to static overpressure impulse, however, further work will be conducted to ensure sensor repeatability prior to defining injury severity. Metabolic distress was detected in the hippocampus at 24 hr following a single high impulse event. Future work will investigate

temporal metabolic profiles at 1 hr, 4 hr, 24 hr, and 48 hr following high impulse events where we aim to translate this work *in vivo* using MRS to confirm these metabolic profiles. Once the profiles have been established, therapeutic targets can be identified and diagnostic measures using MRS in humans following space travel can be implemented to ensure the neurological safety of current and future explorers.

Acknowledgements

The authors would like to thank Dr. James C. DeMar and Janice Mayer for assistance with HPLC optimization and Dave Ritzel for his assessment of intracranial pressure sensor inconsistencies. We also want to thank the Virginia Space Grant Consortium and the Institute for Critical Technology and Applied Science at Virginia Tech for funding this research.

References

1. Jandial, R., et al., *Space-brain: The negative effects of space exposure on the central nervous system.* Surgical neurology international, 2018. **9**: p. 9-9.

2. Parihar, V.K., et al., *What happens to your brain on the way to Mars.* Science Advances, 2015. **1**(4): p. e1400256.

3. Marshall-Goebel, K., R. Damani, and E.M. Bershad, *Brain Physiological Response and Adaptation During Spaceflight.* Neurosurgery, 2019. **85**(5): p. E815-E821.

4. Michael, A.P. and K. Marshall-Bowman, *Spaceflight-Induced Intracranial Hypertension.* Aerospace Medicine and Human Performance, 2015. **86**(6): p. 557-562.

5. Hardy, W.N., et al., *A study of the response of the human cadaver head to impact.* Stapp car crash journal, 2007. **51**: p. 17-80.

6. Ward, C., M. Chan, and A. Nahum, *Intracranial Pressure — A Brain Injury Criterion.* SAE Transactions, 1980. **89**: p. 3867-3880.

7. Guerriero, R.M., C.C. Giza, and A. Rotenberg, *Glutamate and GABA imbalance following traumatic brain injury.* Curr Neurol Neurosci Rep, 2015. **15**(5): p. 27.

8. Rothman, D.L., et al., *In vivo NMR studies of the glutamate neurotransmitter flux and neuroenergetics: implications for brain function.* Annu Rev Physiol, 2003. **65**: p. 401-27.

9. Bak, L.K., A. Schousboe, and H.S. Waagepetersen, *The glutamate/GABA-glutamine cycle: aspects of transport, neurotransmitter homeostasis and ammonia transfer.* J Neurochem, 2006. **98**(3): p. 641-53.

10. Simon, G., J.B. Drori, and M.M. Cohen, *Mechanism of conversion of aspartate into glutamate in cerebral-cortex slices.* The Biochemical journal, 1967. **102**(1): p. 153-162.

11. Lee, S.-H., et al., *Neurophysiology of space travel: energetic solar particles cause cell type-specific plasticity of neurotransmission.* Brain structure & function, 2017. **222**(5): p. 2345-2357.

12. Cho, H.J., et al., *Blast induces oxidative stress, inflammation, neuronal loss and subsequent short-term memory impairment in rats.* Neuroscience, 2013. **253**: p. 9-20.

13. Zhang, Q., et al., *Fast UHPLC Methods for Analysis of Amino Acids*, in *PITTCON Conference and Expo*. 2013: Philadelphia, PA.

14. Leonardi, A.D., et al., *Intracranial pressure increases during exposure to a shock wave.* J Neurotrauma, 2011. **28**(1): p. 85-94.

15. Bolander, R., et al., *Skull Flexure as a Contributing Factor in the Mechanism of Injury in the Rat when Exposed to a Shock Wave.* Annals of Biomedical Engineering, 2011. **39**(10): p. 2550.

16. Sajja, V.S.S.S., et al., *Blast-induced neurotrauma leads to neurochemical changes and neuronal degeneration in the rat hippocampus.* NMR in Biomedicine, 2012. **25**(12): p. 1331-1339.

17. Lee, J. and G. Rude, *Methodologies and gauges for intracranial pressure measurements*, in *Personal Armour Systems Symposium (PASS)*. 2016: Amsterdam, Netherlands.

18. Walls, A.B., et al., *The Glutamine–Glutamate/GABA Cycle: Function, Regional Differences in Glutamate and GABA Production and Effects of Interference with GABA Metabolism.* Neurochemical Research, 2015. **40**(2): p. 402-409.

19. Rana, P., et al., *Oxidative stress contributes to cerebral metabolomic profile changes in animal model of blast-induced traumatic brain injury.* Metabolomics, 2020. **16**(3): p. 39.

20. Amorini, A.M., et al., *Severity of experimental traumatic brain injury modulates changes in concentrations of cerebral free amino acids.* J Cell Mol Med, 2017. **21**(3): p. 530-542.